DOI: 10.1002/ange.201307889

Heme Proteins

Inhibition of Heme Uptake in *Pseudomonas aeruginosa* by its Hemophore ($HasA_p$) Bound to Synthetic Metal Complexes**

Chikako Shirataki, Osami Shoji, Mitsuyoshi Terada, Shin-ichi Ozaki, Hiroshi Sugimoto, Yoshitsugu Shiro, and Yoshihito Watanabe**

Abstract: *The heme acquisition system A protein secreted by Pseudomonas aeruginosa ($HasA_p$) can capture several synthetic metal complexes other than heme. The crystal structures of $HasA_p$ harboring synthetic metal complexes revealed only small perturbation of the overall $HasA_p$ structure. An inhibitory effect upon heme acquisition by $HasA_p$ bearing synthetic metal complexes was examined by monitoring the growth of Pseudomonas aeruginosa PAO1. $HasA_p$ bound to iron–phthalocyanine inhibits heme acquisition in the presence of heme-bound $HasA_p$ as an iron source.*

The heme acquisition system A (HasA) protein is a hemophore secreted by some pathogenic bacteria with a heme acquisition (Has) system such as *Pseudomonas aeruginosa*,[1] *Serratia marcescens*,[2] *Pseudomonas fluorescens*,[3] and *Yersinia pestis*[3b,4] (Figure 1). Under the low-iron conditions found in animal cells, these bacteria secrete HasA to capture heme from their hosts as an iron source.[2b] The heme captured by HasA is transferred to a hemophore-specific outer-membrane receptor called HasR.[5] HasA-type hemophores have attracted much attention for their heme acquisition from target hemoproteins such as hemoglobin in the hosts[2b] and for the transfer of heme from HasA to HasR.[6] The crystal structure of the heme-bound form (holo form) of the hemophore from *S. marcescens* ($HasA_{sm}$) was first solved by Arnoux et al.[7] $HasA_{sm}$ binds heme through two loops with coordination of Tyr75 and His32 to the heme iron center.[7] The overall structure of $HasA_{sm}$ bound to heme resembles "a fish biting the heme".[7] Subsequently, Alontaga et al. reported the crystal structure of the hemophore from *P. aeruginosa* ($HasA_p$).[8] The structures of these two hemophores are essentially identical.

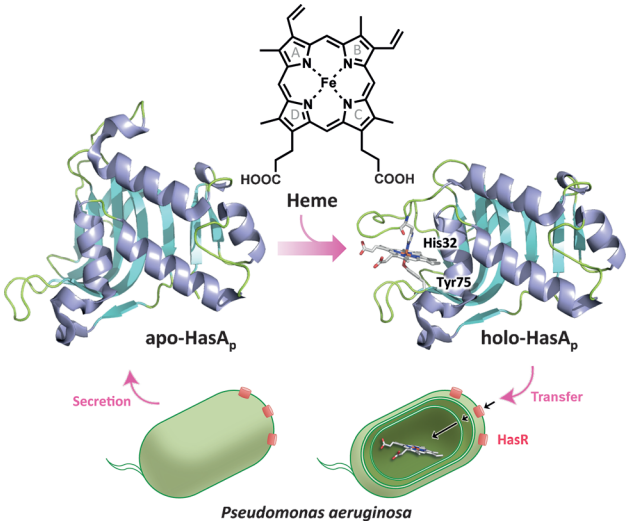

Figure 1. The Has system in *P. aeruginosa*. Under low-iron conditions, *P. aeruginosa* secretes apo-$HasA_p$ (PDB ID: 3MOK), which captures heme (PDB ID: 3ELL); the resulting holo-$HasA_p$ delivers the captured heme to the specific outer membrane receptor, HasR, on *P. aeruginosa*. In holo-$HasA_p$, His32 and Tyr75 coordinate to the heme iron atom. In the bound heme, the edges of the pyrrole rings A, C and D are highly solvent exposed.

The crystal structures of the holo forms of HasA proteins show that the captured heme moiety is highly solvent exposed; not only the propionate groups but also the edges of the heme pyrrole rings A, C, and D can be seen from outside (Figure 1). This unique fashion of heme binding, like a pair of tweezers griping the heme, suggests that metal complexes with different structures to heme could be accommodated by HasA proteins. Because the heme-free form (apo form) of HasA exhibits an open conformation with a large rearrangement of the His-32 loop (Figure 1),[9] even relatively bulky metal complexes could enter the heme

[*] Prof. Dr. Y. Watanabe
Research Center for Materials Science, Nagoya University
Furo-cho, Chikusa-ku, Nagoya 464-8602 (Japan)
E-mail: p47297a@nucc.cc.nagoya-u.ac.jp
Homepage: http://bioinorg.chem.nagoya-u.ac.jp/
C. Shirataki, Dr. O. Shoji, M. Terada
Department of Chemistry, Graduate School of Science
Nagoya University, Furo-cho, Chikusa-ku, Nagoya 464-8602 (Japan)
E-mail: shoji.osami@a.mbox.nagoya-u.ac.jp
Prof. Dr. S. Ozaki
Department of Biological Science, Yamaguchi University
1677-1 Yoshida, Yamaguchi 753-8515 (Japan)
Dr. H. Sugimoto, Prof. Dr. Y. Shiro
RIKEN SPring-8 Center, Harima Institute
1-1-1 Kouto, Sayo, Hyogo 679-5148 (Japan)

[**] This work was supported by Grants-in-Aid for Scientific Research (S) to Y. W. (24225004), Grant-in-Aid for Scientific Research on Innovative Areas "Molecular Activation Directed toward Straightforward Synthesis" to Y. S. (22105012) and to O. S. (25105724), and a Grant-in-Aid for Young Scientists (A) to O.S. (21685018) from the Ministry of Education, Culture, Sports, Science, and Technology (MEXT) (Japan). C.S. was supported by Global COE Program "Elucidation and Design of Materials and Molecular Functions" and the Program for Leading Graduate Schools "Integrative Graduate Education and Research Program in Green Natural Sciences" by MEXT (Japan). We thank Dr. Go Ueno, Dr. Yuki Nakamura, Dr. Hironori Murakami, and Dr. Nobuyuki Shimizu for their assistance with the data collection at SPring-8.

Supporting information for this article is available on the WWW under http://dx.doi.org/10.1002/anie.201307889.

binding pocket. These considerations led us to investigate whether HasA could capture metal complexes other than heme. We were also interested in how the addition of synthetic metal complexes to HasA might affect the transfer of heme from HasA to HasR. We report herein that the hemophore from *P. aeruginosa* ($HasA_p$) can capture several metal complexes including Fe–phthalocyanine (Fe–Pc) without any structural perturbation and the resulting Fe–Pc-bound $HasA_p$ markedly inhibits the growth of *P. aeruginosa* even in the presence of heme-bound $HasA_p$.

First, we investigated whether $HasA_p$ interacts with synthetic metal complexes that have different structures to heme by subjecting a simple mixture of 3.5 μM apo-$HasA_p$ and a methanolic solution of metal complexes (2.7 equiv) to electrospray ionization time-of-flight mass spectrometry (ESI-TOF-MS; (Figure 2a–e). With heme, the intensity ratio of apo-$HasA_p$ to holo-$HasA_p$ was 1:0.6 under the conditions examined (Cone voltage: 45 V). Under similar conditions, the synthetic metal complexes iron mesoporphyrin IX (Fe–MPIX), iron 2,3,7,8,12,13,17,18-octaethyl-21H,23H-porphyrin (Fe–OEP), and iron *N*,*N*′-disalicylal-1,2-phenylenediamine (Fe–salophen) gave peaks corresponding to holo-$HasA_p$ formation, whereas iron tetraphenylporphyrin (Fe–TPP) showed only the peak for apo-$HasA_p$ (Figure 2a–e). The intensity of the peaks for holo-$HasA_p$ bound to these metal complexes was comparable to or even larger than that measured with heme, thus indicating that the complexes of $HasA_p$ with Fe–MPIX, Fe–OEP, or Fe–salophen are relatively stable[10] (Figure 2a–e, the UV/Vis spectra of samples used for ESI-TOF-MS are shown in Figure S1 in the Supporting Information). In fact, we have succeeded in purifying $HasA_p$ bound to these metal complexes by column chromatography.

UV/Vis spectra of $HasA_p$ bound to metal complexes after purification are shown in Figure S2. A titration experiment showed 1:1 binding of $HasA_p$ and the metal complexes (see Figure S3). These results suggest that $HasA_p$ can capture these metal complexes, which have a planar structure, in the same fashion as with heme. We have further succeeded in crystalizing $HasA_p$ bound to Fe–salophen and Fe–MPIX (Figure 3a,b). The crystal structures show clear electron densities assignable to Fe–salophen (Figure 3d) and Fe–MPIX (Figure 3e) at the heme-binding position. The overall structures of Fe–salophen-bound $HasA_p$ and Fe–MPIX-bound $HasA_p$ are essentially identical to that of heme-bound $HasA_p$ (root-mean-square deviation (RMSD) over 2–184 amino acid residues for Cα atoms: 0.810 for Fe–salophen and 0.443 for Fe–MPIX), whereas the His32 loop in Fe–salophen-bound $HasA_p$ is clearly shifted inwards as a result of induced-fit binding to accommodate a small metal complex (Figure S4). Both Tyr75 and His32 bind to the iron atoms of Fe–salophen and Fe–MPIX. The location of Fe–MPIX is identical to that of heme but Fe–MPIX is captured in a reverse orientation relative to that of heme (minor orientation; Figure 3k and Figure S4), possibly as a result of steric repulsion between the two ethyl groups of Fe–MPIX, which protrude out of the porphyrin plane. This observation indicates that heme binding by $HasA_p$ is regulated by recognition of the vinyl groups of the heme so that heme can only be bound in a single orientation. Although the structure of Fe–salophen is largely different from heme, Fe–salophen was similarly captured by $HasA_p$. The central phenyl ring of the salophen ligand was accommodated in the hydrophobic pocket composed of Phe46, Tyr56, Leu85, His134, Val137, and Met141 located deep in the heme binding site (Figure 3g). This interaction seems to be a key interaction in the binding of Fe–salophen and leads to a single orientation of Fe–salophen in $HasA_p$.

Given the crystal structure of $HasA_p$ bound to Fe–salophen, it is intriguing to examine binding of Fe–phthalocyanine (Fe–Pc) to $HasA_p$ because the structure of Fe–Pc is similar to that of Fe–salophen and the crystal structures shown in Figure 3 suggest that there is enough space to accommodate Fe–Pc, which bears a large π-plane. Phthalocyanine is a highly hydrophobic molecule with a large planar structure and is thus insoluble in water; it is even difficult to

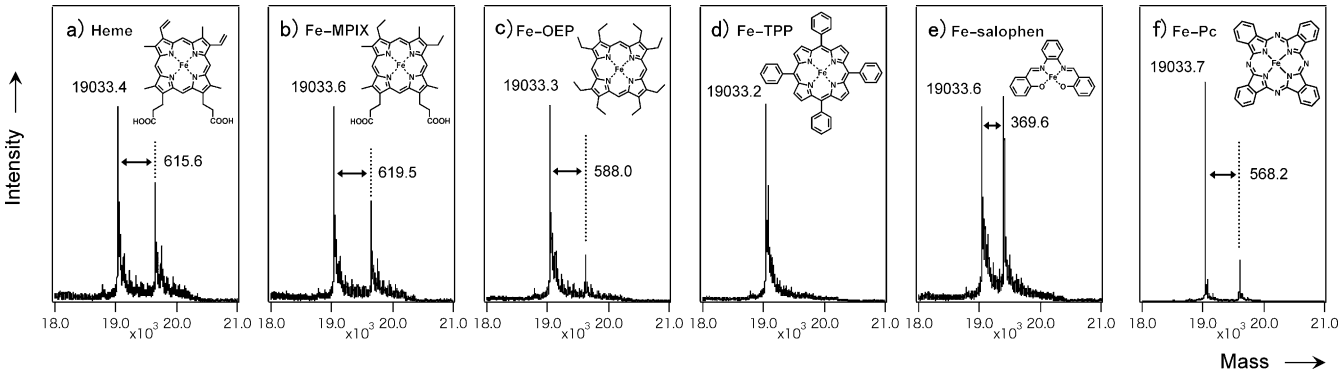

Figure 2. Positive mode ESI-TOF-MS spectra of the mixtures of apo-$HasA_p$ and the metal complexes: a) hemin; b) Fe–MPIX·Cl; c) Fe–OEP·Cl; d) Fe–TPP·Cl; and e) Fe–salophen·Cl. The sample mixture was prepared by adding 100 μL (2.7 equiv) of metal complexes dissolved in methanol to a solution of purified apo-$HasA_p$ in ammonium acetate buffer (5 mM, 3.5 nmol, 900 μL). Cone voltage was fixed at 45 V. The molecular weight of apo-$HasA_p$ was calculated to be 19034.77 Da based on its amino acid sequence. f) Positive mode ESI-TOF mass spectrum of purified $HasA_p$ harboring Fe–Pc in 5 mM ammonium acetate buffer. The concentration of $HasA_p$ with Fe–Pc was 4.5 μM. The exact masses of the metal complexes are 616.18 Da (heme), 620.21 Da (Fe–MPIX), 588.29 Da (Fe–OEP), 668.17 Da (Fe–TPP), 370.04 Da (Fe–salophen), and 568.08 Da (Fe–Pc).

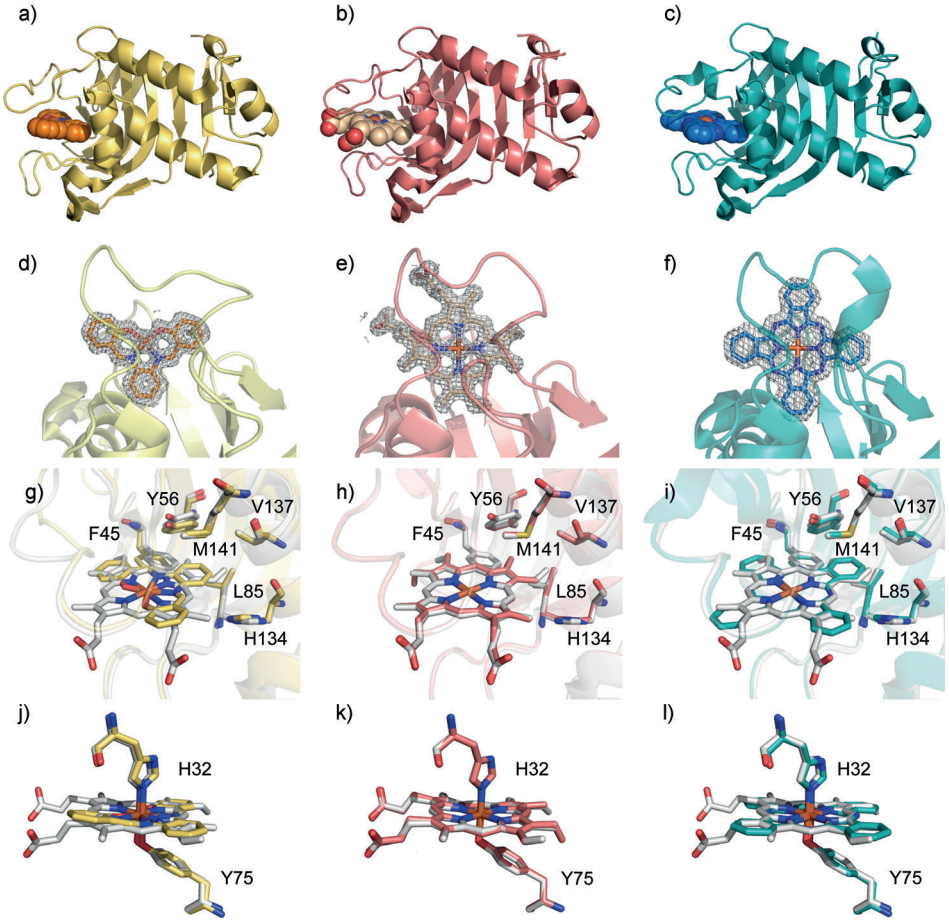

Figure 3. X-ray crystal structures of $HasA_p$ with synthetic metal complexes: Fe–salophen (yellow; a, d, g, j); Fe–MPIX (pink; b, e, h, k); and Fe–Pc (turquoise; c, f, i, l). In the side views of overall structures (top row, a–c) $HasA_p$ is shown as a ribbon model and the metal complexes as space filling models. In the top views of the binding sites (second row, d–f), $HasA_p$ is shown as a ribbon model and 2 F_o-F_c electron-density maps of the metal complexes contoured at the 1.0σ level are shown in gray mesh. In the third row (g–i), close-up views corresponding to those from the propionate side of the heme are shown, with the metal complexes and the hydrophobic amino acid residues located in the binding pocket depicted as stick models. Close-up views of the side of the metal complexes are shown in the bottom row (j–l), with H32, Y75 and the metal complexes shown as stick models. In the bottom two rows, the crystal structure of heme-bound $HasA_p$ (PDB ID: 3ELL) is superimposed on the stick models and depicted in light gray. The electron densities from F_o-F_c Fourier synthesis omitting the metal complexes are presented in the Figure S5. The atomic coordinates and structure factors (codes 3W8M, 3WAH, and 3W8O) have been deposited in the Protein Data Bank.

dissolve Fe–Pc in methanol, mainly because of a strong stacking interaction. We thus had to use other polar organic solvents to dissolve the Fe–Pc. Because apo-$HasA_p$ did not aggregate even in 50% DMSO, we used a DMSO solution of Fe–Pc to examined the binding of Fe–Pc to apo-$HasA_p$. Fe–Pc-bound $HasA_p$ was stable even after the removal of DMSO by dialysis (Figure 2f, Figure S2). The crystal structure of Fe–Pc-bound $HasA_p$ showed clear electron density for Fe–Pc and the binding fashion was similar to that of Fe–salophen (Figure 3f). As was observed for Fe–salophen binding, one of the phenyl rings of Fe–Pc was accommodated in the hydrophobic pocket in the depths of the heme binding site (Figure 3i). Only minor perturbation of the overall structure of $HasA_p$ was observed (Figure 3c and Figure S4). The RMSD over 2–184 amino acid residues for Cα atoms against heme-bound $HasA_p$ was estimated to be 0.915.

To examine the effect of synthetic metal complexes on the growth of *P. aeruginosa*, we cultured *P. aeruginosa* PAO1 in the presence of $HasA_p$ bound to the artificial metal complexes and monitored bacterial growth through measuring the absorbance of the culture at 600 nm (OD_{600}; Figure 4a). Even though *P. aeruginosa* did not grow in a medium containing EDTA as an iron ion scavenger (Figure 4a, green line), *P. aeruginosa* started to grow following the addition of heme-bound $HasA_p$ to the medium (Figure 4a, red line), thus indicating that *P. aeruginosa* uses the heme in holo-$HasA_p$ as an iron source. Growth of *P. aeruginosa* was also observed following the addition of Fe–MPIX-bound $HasA_p$ (Figure 4a, pink line), thus indicating that *Pseudomonas aeruginosa* could utilize Fe–MPIX as an iron source. These results show that the transfer of heme from $HasA_p$ to HasR as well as the heme degradation processes to acquire iron[11] are not much affected by the substitution of the two vinyl groups for ethyl groups. By contrast, for $HasA_p$ bound to Fe–salophen or Fe–Pc, the OD_{600} values did not increase. This suggests either that Fe–salophen and Fe–Pc are not transferred to HasR or that they are transferred to HasR but the subsequent steps were inhibited (Figure 4c, Steps III, IV, and V).

To examine the influence of Fe–salophen and Fe–Pc on the growth of *P. aeruginosa*, we cultured the bacteria in media containing both $HasA_p$ bound to heme and $HasA_p$ bound to Fe–salophen or Fe–Pc. Interestingly, in the presence of Fe–Pc-bound $HasA_p$, the OD_{600} values did not increase at all despite the presence of heme-bound $HasA_p$ (Figure 4b, blue line). $HasA_p$ bound to Fe–salophen did not affect the growth of *P. aeruginosa* under these conditions. These results clearly indicate that $HasA_p$ bound to Fe–Pc inhibits heme acquisition by the Has system. The half-maximal inhibitory concentration (IC_{50}) was estimated to be 24 nM, thus indicating that Fe–Pc-bound $HasA_p$ efficiently inhibited heme transportation (Figure S6). No toxicity for the cells of $HasA_p$ bound to Fe–Pc was

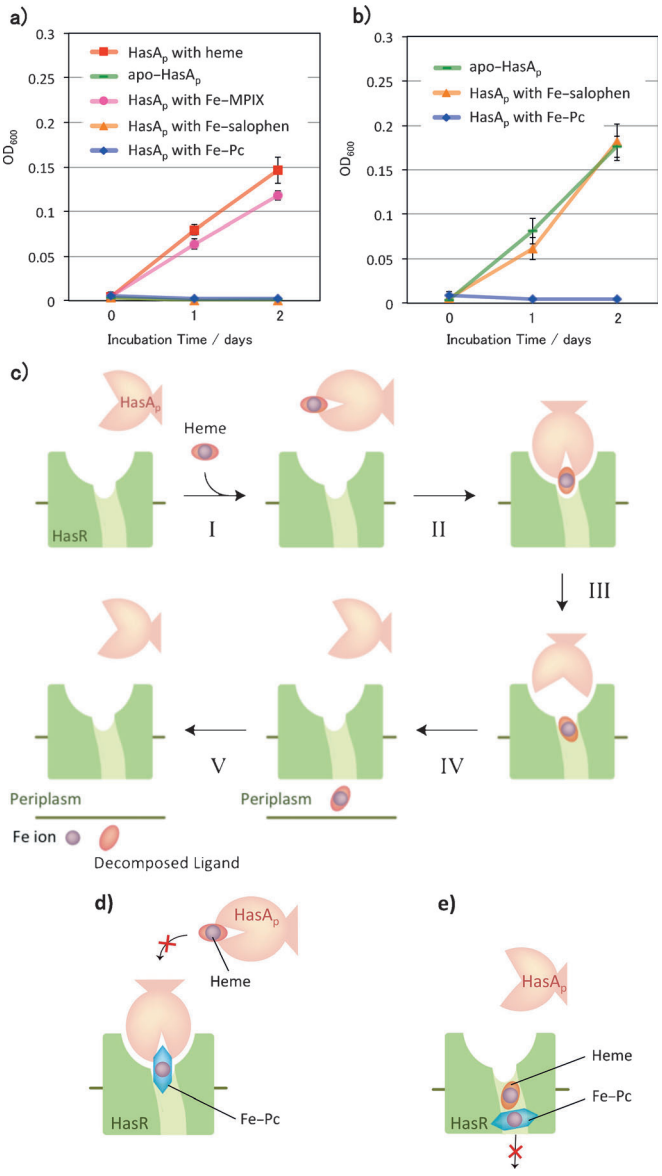

Figure 4. Growth behavior of *P. aeruginosa* in iron-limited medium containing EDTA as a scavenger of iron cations. Cell growth was monitored through optical density at 600 nm (OD_{600}). a) Growth of *P. aeruginosa* in the presence of 0.25 μM of heme-bound holo-HasA$_p$ or HasA$_p$ bound to synthetic metal complexes. As a control experiment, apo-HasA$_p$ was also tested (green line). b) The effect of HasA$_p$ bound to synthetic metal complexes on the growth of *P. aeruginosa* in the presence of heme-bound HasA$_p$. A solution of HasA$_p$ bound to synthetic metal complexes or apo-HasA$_p$ (as a negative control) was added to a suspension of *P. aeruginosa* (the final concentrations were 0.25 μM) provided with 0.5 μM heme-bound holo-HasA$_p$ as an iron source. Error bars represent the standard deviation of at least three measurements. c) Steps of the general heme uptake process by HasA. HasA captures a heme molecule (step I). Holo-HasA then interacts with a specific receptor called HasR (step II) and the heme is transferred from HasA to HasR (step III). The heme passes through HasR and is transported into the periplasm (step IV). The heme is degraded by an enzyme to release an iron cation in the cytoplasm (step V). d) and e) Schematic representations of plausible mechanisms to explain the inhibition of HasA$_p$-mediated heme uptake by Fe–Pc-bound HasA$_p$: HasA$_p$ bound to Fe–Pc strongly interacts with HasR and blocks the specific interaction domain of HasR (d); or Fe–Pc is transferred to HasR and blocks the access channel (e).

observed: there was no growth inhibition by Fe–Pc-bound HasA$_p$ either in the absence of EDTA (i.e., in iron-containing medium) or in the presence of free Hemin (Figure S7 and S8). Although further studies on the interaction between HasA$_p$ and HasR, including the transfer of metal complexes from HasA$_p$ to HasR, are required to clarify the mechanism of inhibition by HasA$_p$ bound to Fe–Pc, we propose two possibilities: 1) Fe–Pc-bound HasA$_p$ strongly interacts with HasR and blocks the specific interaction domain of HasR, thereby resulting in a strong inhibition of heme transfer from holo-HasA$_p$ to HasR (step III in Figure 4c, Figure 4d); 2) Fe–Pc is transferred to HasR and blocks the access channel of HasR because of the higher hydrophobicity of Fe–Pc compared to heme (step IV in Figure 4c, Figure 4e). Fe–salophen-bound HasA$_p$ did not inhibit the growth of *P. aeruginosa*, thus suggesting that Fe–salophen bound to HasA could not block the specific interaction domain of HasR or that transferred Fe–salophen was not effective in blocking the access channel of HasR. It is very interesting that the inhibitory effect differs depending on the structure of the metal complexes captured by HasA$_p$.

In conclusion, we have demonstrated that HasA$_p$ can capture several synthetic metal complexes other than heme. The crystal structures of HasA$_p$ bound to Fe–MPIX, Fe–salophen, and Fe–Pc showed that HasA$_p$ captures these metal complexes in the same fashion as it does heme without any structural perturbation. We also found that HasA$_p$ bound to Fe–Pc strongly inhibited HasA$_p$-mediated heme acquisition. These findings contribute to the understanding of heme transfer from HasA to HasR. Furthermore, we expect that these observations could lead to the development of a *P. aeruginosa* elimination system that doesn't involve antibiotics.

Received: September 7, 2013
Revised: December 30, 2013
Published online: February 7, 2014

Keywords: growth inhibition · HasA · heme proteins · iron complexes · protein structures

[1] S. Letoffe, V. Redeker, C. Wandersman, *Mol. Microbiol.* **1998**, *28*, 1223–1234.
[2] a) J. M. Ghigo, S. Letoffe, C. Wandersman, *J. Bacteriol.* **1997**, *179*, 3572–3579; b) S. Letoffe, J. M. Ghigo, C. Wandersman, *Proc. Natl. Acad. Sci. USA* **1994**, *91*, 9876–9880.
[3] a) A. Idei, E. Kawai, H. Akatsuka, K. Omori, *J. Bacteriol.* **1999**, *181*, 7545–7551; b) S. Letoffe, K. Omori, C. Wandersman, *J. Bacteriol.* **2000**, *182*, 4401–4405.
[4] R. Kumar, S. Lovell, H. Matsumura, K. P. Battaile, P. Moenne-Loccoz, M. Rivera, *Biochemistry* **2013**, *52*, 2705–2707.
[5] S. Létoffé, C. Deniau, N. Wolff, E. Dassa, P. Delepelaire, A. Lecroisey, C. Wandersman, *Mol. Microbiol.* **2001**, *41*, 439–450.
[6] a) S. Krieg, F. Huche, K. Diederichs, N. Izad *i*Pruneyre, A. Lecroisey, C. Wandersman, P. Delepelaire, W. Welte, *Proc. Natl. Acad. Sci. USA* **2009**, 106, 1045–1050; b) N. Izad *i*Pruneyre, F. Huche, G. S. Lukat-Rodgers, A. Lecroisey, R. Gilli, K. R. Rodgers, C. Wandersman, P. Delepelaire, *J. Biol. Chem.* **2006**, 281, 25541–25550.
[7] P. Arnoux, R. Haser, N. Izadi, A. Lecroisey, M. Delepierre, C. Wandersman, M. Czjzek, *Nat. Struct. Biol.* **1999**, *6*, 516–520.

[8] A. Y. Alontaga, J. C. Rodriguez, E. Schonbrunn, A. Becker, T. Funke, E. T. Yukl, T. Hayashi, J. Stobaugh, P. Moenne-Loccoz, M. Rivera, *Biochemistry* **2009**, *48*, 96 – 109.
[9] a) G. Jepkorir, J. C. Rodriguez, H. A. Rui, W. Im, S. Lovell, K. P. Battaile, A. Y. Alontaga, E. T. Yukl, P. Moenne-Loccoz, M. Rivera, *J. Am. Chem. Soc.* **2010**, *132*, 9857 – 9872; b) N. Wolff, N. Izad *i*Pruneyre, J. Couprie, M. Habeck, J. Linge, W. Rieping, C. Wandersman, M. Nilges, M. Delepierre, A. Lecroisey, *J. Mol. Biol.* **2008**, 376, 517 – 525.
[10] Y. Satake, S. Abe, S. Okazaki, N. Ban, T. Hikage, T. Ueno, H. Nakajima, A. Suzuki, T. Yamane, H. Nishiyama, Y. Watanabe, *Organometallics* **2007**, *26*, 4904 – 4908.
[11] M. Ratliff, W. M. Zhu, R. Deshmukh, A. Wilks, I. Stojiljkovic, *J. Bacteriol.* **2001**, *183*, 6394 – 6403.

